Acta Crystallographica Section D
Biological Crystallography
ISSN 0907-4449

Crystal structures of two peptide–HLA-B*1501 complexes; structural characterization of the HLA-B62 supertype

Gustav Røder,[a]* Thomas Blicher,[b] Sune Justesen,[a] Birthe Johannesen,[c] Ole Kristensen,[c] Jette Kastrup,[c] Søren Buus[a] and Michael Gajhede[c]

[a]Institute of Medical Microbiology and Immunology, Panum Institute 18.3.20, Blegdamsvej 3B, 2200N Copenhagen, Denmark, [b]Center for Biological Sequence Analysis, BioCentrum-DTU, Technical University of Denmark, Kemitorvet, Building 208, 2800 Lyngby, Denmark, and [c]Department of Medicinal Chemistry, The Danish University of Pharmaceutical Sciences, Universitetsparken 2, 2100 Copenhagen, Denmark

Correspondence e-mail: g.roder@immi.ku.dk

Received 25 April 2006
Accepted 17 July 2006

PDB References:
LEKARGSTY, 1xr8, r1xr8sf; ILGPPGSVY, 1xr9, r1xr9sf.

MHC class I molecules govern human cytotoxic T cell responses. Their specificity determines which peptides they sample from the intracellular protein environment and then present to human cytotoxic T cells. More than 1100 different MHC class I proteins have been found in human populations and it would be a major undertaking to address each of these specificities individually. Based upon their peptide binding specificity, they are currently subdivided into 12 supertypes. Several of these HLA supertypes have not yet been described at the structural level. To support a comprehensive understanding of human immune responses, the structure of at least one member of each supertype should be determined. Here, the structures of two immunogenic peptide–HLA-B*1501 complexes are described. The structure of HLA-B*1501 in complex with a peptide (LEKARGSTY, corresponding to positions 274–282 in the Epstein–Barr virus nuclear antigen-3A) was determined to 2.3 Å resolution. The structure of HLA-B*1501 in complex with a peptide (ILGPPGSVY) derived from human ubiquitin-conjugating enzyme-E2 corresponding to positions 91–99 was solved to 1.8 Å resolution. Mutual comparisons of these two structures with structures from other HLA supertypes define and explain the specificity of the P2 and P9 peptide anchor preferences in the B62 HLA supertype. The P2 peptide residue binds to the B-pocket in HLA-B*1501. This pocket is relatively large because of the small Ser67 residue located at the bottom. The peptide proximal part of the B-pocket is hydrophobic, which is consistent with P2 anchor residue preference for Leu. The specificity of the B-pocket is determined by the Met45, Ile66 and Ser67 residues. The apex of the B-pocket is hydrophilic because of the Ser67 residue. The P9 peptide residue binds to the F-pocket in HLA-B*1501. The residues most important for the specificity of this pocket are Tyr74, Leu81, Leu95, Tyr123 and Trp147. These residues create a hydrophobic interior in the F-pocket and their spatial arrangement makes the pocket capable of containing large, bulky peptide side chains. Ser116 is located at the bottom of the F-pocket and makes the bottom of this pocket hydrophilic. Ser116, may act as a hydrogen-bonding partner and as such is a perfect place for binding of a Tyr9 peptide residue. Thus, based on structure information it is now possible to explain the peptide sequence specificity of HLA-B*1501 as previously determined by peptide binding and pool sequencing experiments.

1. Introduction

Specific cellular immune responses are largely governed by molecules of the major histocompatibility complex (MHC, or in humans: HLA). The development of specific cytotoxic T cell (CTL) responses is crucially dependent upon MHC-I

molecules. Their function is to sample peptides derived from the protein metabolism of our cells and display them at the cell surface, where they can be examined by CTLs (reviewed in Guermonprez *et al.*, 2002). In brief, MHC-I molecules translocate information about the antigenic contents of our cells, from the inside where intracellular pathogens (*e.g.* viruses) reside to the outside where CTLs are found (reviewed in Heemels & Ploegh, 1995). This enables CTLs to scrutinize the interior of the cells and attack those cells harboring intracellular pathogens. MHC-I function and specificity are critical factors in generating and maintaining immune protection against intracellular pathogens and therefore an important consideration in the development of effective immunotherapy including vaccination (Lauemøller *et al.*, 2000; Yewdell *et al.*, 1999).

The specificity of MHC-I molecules determines which peptides will be presented and potentially recognized by the immune system. If only one MHC-I specificity existed in the human population, this would amount to a constant pressure upon human pathogens to remove immune epitopes and eventually it would lead to the evolution of stealth pathogens. To avoid this conundrum, the immune system has developed many different MHC-I specificities. More than 1100 different MHC class I proteins have been found and registered in human populations (albeit each individual only expresses a few of these specificities) making MHC-I the most polymorphic gene system known to mankind. Biologically, this extreme diversity individualizes MHC-I restricted immune responses effectively avoiding a constant evolutionary pressure to remove any specific immune epitope. However, experimentally, this polymorphism is a huge logistic challenge. In an attempt to reduce the complexity, it has been suggested to group MHC-I specificities into 12 HLA supertypes (A1, A2, A3, A24, A26, B7, B8, B27, B39, B40, B58 and B62) each representing a peptide-binding specificity largely shared between different members of the same supertype and differing from members of other supertypes (Lund *et al.*, 2004; Sette & Sidney, 1999; Sylvester-Hvid *et al.*, 2004). These supertypes cover more than 99% of all individuals of all major human populations.

We and others have proposed that a detailed understanding of peptide–MHC interactions should be achieved, as it eventually will enable a rational exploitation of human immune responses (Sette *et al.*, 2005). This should include quantitative data and computational predictive algorithms allowing entire genomes to be rapidly and accurately screened for potential immunogenic epitopes (Lauemøller *et al.*, 2000; Tscharke *et al.*, 2005). At this time, predictions of peptide binding rely mostly on searching target proteins for the presence of sequence motifs; a strategy which uses matrices and assumes sequence independence. Previous structure analyses of peptide–MHC interactions have demonstrated that this assumption represents an oversimplification and that one amino-acid residue, when present at a specific position, may affect the recognition at other positions; *i.e.* binding includes correlated effects, which cannot be represented in a straightforward matrix-driven prediction. A more recently adopted strategy used artificial neural networks (ANN), which allow for pattern recognition and incorporate correlated effects (Christensen *et al.*, 2003). Although ANN represents advancement towards predictions of peptide–MHC interaction, it is still crucially dependent upon the availability of structure data, which currently can only be generated at considerable expense. An alternative approach would be to use structural information to predict peptide binders (Rognan *et al.*, 1999). Currently, a major disadvantage of structure-based predictions relates to the calculation-intensive nature of such predictions, which would tend to preclude whole genome screening. On the other hand, if computer technology improves sufficiently one may envision harvesting significant advantages. If one MHC-I molecule can be modeled using a closely related and experimentally determined MHC-I structure, then predictions may be possible even in cases where no actual data are available. Furthermore, it may even be possible to include correlated effects. We have embarked on a major project to describe and predict all major HLA specificities primarily using the ANN approach and at least one member of each supertype should be understood in depth. To support structure-based prediction efforts this should include high-resolution crystal structures as predictions built upon an experimentally determined structure may lead to structure-based predictions that are significantly better than a prediction built upon a model (Rognan *et al.*, 1999).

Currently, no member of the A24, A26, B39, B58 and B62 supertypes have been characterized at the structure level, whereas several crystal structures involving members of the A2 supertype have been determined. The B62 supertype accounts for about 18% of various human populations. Binding peptides of the B62 supertype member HLA-B*1501 preferentially have the aliphatic residues such as Leu in position 2, and the aromatic residues Tyr or Phe at the C-terminus (Barber *et al.*, 1996; Falk *et al.*, 1995; Prilliman *et al.*, 1997). Here, we report the first crystal structures of any member of the B62 supertype, HLA-B*1501. The structures of two peptide–HLA-B*1501 complexes have been determined; one at 1.8 Å resolution involving a known HLA-B*1501-restricted Epstein–Barr Nuclear Antigen-3 (EBNA-3A)-specific CTL peptide epitope (LEKARGSTY) identified in healthy carriers (Rickinson & Moss, 1997); the other at 2.3 Å resolution involving an autologous CTL peptide epitope (ILGPPGSVY) from the human UbcH6 ubiquitin-protein ligase (Barber *et al.*, 1996; Prilliman *et al.*, 1997). The structural basis of the unique B62 specificity is discussed by comparison with structural information from other HLA supertypes.

2. Materials and methods

2.1. Cloning

A genetic construct representing the HLA-B*1501 positions 1–276 was derived by site-directed mutagenesis from an HLA-A*0201 gene using the QuikChange Multi Site-Directed Mutagenesis Kit (Stratagene). This procedure involved 81 nucleotide mutations, which could be directed by 13 DNA

Table 1
Data collection and refinement statistics.

	LEKARGSTY	ILGPPGSVY
Data collection		
Space group	$P2_12_12_1$ (19)	$P2_12_12_1$ (19)
Resolution (Å)	35.00–2.30 (2.42–2.30)†	31.65–.79 (1.87–1.78)
a (Å)	50.58	50.36
b (Å)	81.89	81.39
c (Å)	110.41	109.97
Molecules/AU	1	1
Data processing and refinement		
Total observations	171220	74885
Unique reflections	19549	41032
Completeness (%)	93.2 (96.3)	94.8 (97.4)
R_{merge} (%)	10.4 (33.9)	8.0 (29.8)
Average $I/\sigma(I)$	5.1 (1.9)	7.6 (2.5)
Model		
R (%)	17.3	18.0
R_{free}‡ (%)	24.5	23.2
Mean B (Å)	24.0	20.3
Most favoured (%)	90.8	90.7
Disallowed (%)	0.0	0.0

† Values in parentheses refer to the highest resolution shell. ‡ R_{free} is as R_{cryst}, but calculated on 5% of data excluded from the refinement.

primers. The final HLA-B*1501 sequence was inserted into the pET28a vector (Novagen). The sequence was verified by sequencing (3100 Avant, ABI).

2.2. Protein production and purification

E. coli BL21(DE3) cells were transformed with the HLA-B*1501-pET28 vector and protein was produced in a 2 l fermentor (Infors) by induction with IPTG as previously described (Ferré *et al.*, 2003). Inclusion bodies were obtained by cell disruption (Constant Cell Disruption Systems) and washed twice with PBS containing 0.5%(*v*/*v*) NonIdet-P40/DOC and dissolved in 8 *M* urea and 25 m*M* Tris–HCl (pH 8.0). The urea dissolved HLA-B*1501 protein was further purified by standard chromatography techniques (Akta Prime, Amersham Biosciences) at 285 K. The HLA-B*1501 was separated from endogenous proteins by immobilized metal affinity chromatography using Ni-NTA Sepharose. Buffer *A* contained 8 *M* urea, 100 m*M* NaCl and 25 m*M* Tris–HCl (pH 8.0), and buffer *B* was the same but including 250 m*M* imidazole. A 0–40% gradient in buffer *B* spanning 4 column volumes was applied. The eluted mixture of active HLA-B*1501 disulfide bond isomer was purified by hydrophobic interaction chromatography using Phenyl Sepharose HP. Buffer *A* consisted of 8 *M* urea, 25 m*M* Tris–HCl (pH 8.0) and 100 g l^{-1} ammonium sulfate (Sigma), whereas buffer *B* was 8 *M* urea and 25 m*M* Tris–HCl (pH 8.0). A 0–40% gradient in buffer *B* spanning 6 column volumes was applied. Finally, the HLA-B*1501 sample was purified by size-exclusion chromatography (SEC) on a Sephacryl-S200 in 8 *M* urea, 25 m*M* Tris–HCl (pH 8.0) and 150 m*M* NaCl, and subsequently stored at 253 K.

2.3. Peptide production and purification

The LEKARGSTY and ILGPPGSVY peptides were synthesized by conventional Fmoc chemistry and subsequently purified by reverse-phase HPLC (Schafer-N, Copenhagen). The peptide identities were verified by reverse-phase HPLC followed by ion-trap mass spectrometry (Bruker Daltonics). Their purity was determined to be 83% and 99%, respectively.

2.4. MHC-I complex assembly

For complex assembly, 3 mg denatured HLA-B*1501 heavy chain was rapidly diluted in 1 l of 50 m*M* Tris–HCl (pH 7.5), 3 m*M* EDTA and 150 m*M* NaCl already containing 2 mg β_2-microglobulin (β_2m) and 1 mg peptide (the final concentrations being 100, 170 and 1000 n*M*, respectively). The reaction mixture was incubated at 291 K for 48 h and then concentrated to 10 ml using a pressure cell (Amicon) equipped with a 10 kDa cutoff filter. The highly concentrated mixture was allowed to settle overnight and was subsequently concentrated to 0.5 ml on a 10 kDa spin filter. Folded MHC-I complex was separated from aggregated HLA-B*1501 heavy chain, free β_2m and peptide by Superdex-200 (Amersham Biosciences) SEC. The fractions were analyzed by SDS–PAGE and ion-trap mass spectrometry (data not shown) and fractions containing correctly folded HLA-B*1501 (verified by the presence of HLA-B*1501 heavy chain, β_2m and specific

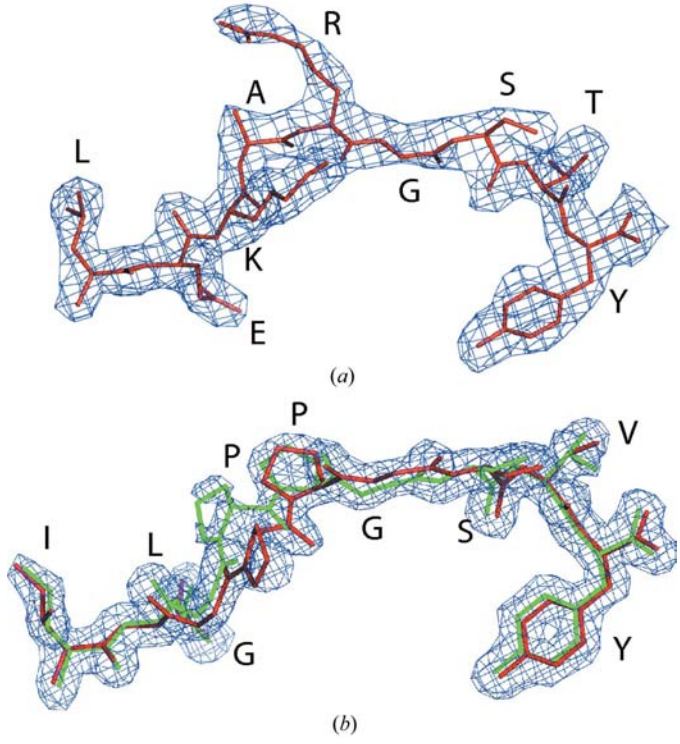

Figure 1
ARP/wARP electron-density maps before manual inclusion of the (*a*) LEKARGSTY and (*b*) ILGPPGSVY peptides from the HLA-B*1501 complexes. The peptide N-termini are located at the left and one-letter amino-acid codes are used. The A-conformation of the ILGPPGSVY peptide is shown in red, while the B-conformation is shown in green. The electron densities are rendered at 1.0σ level.

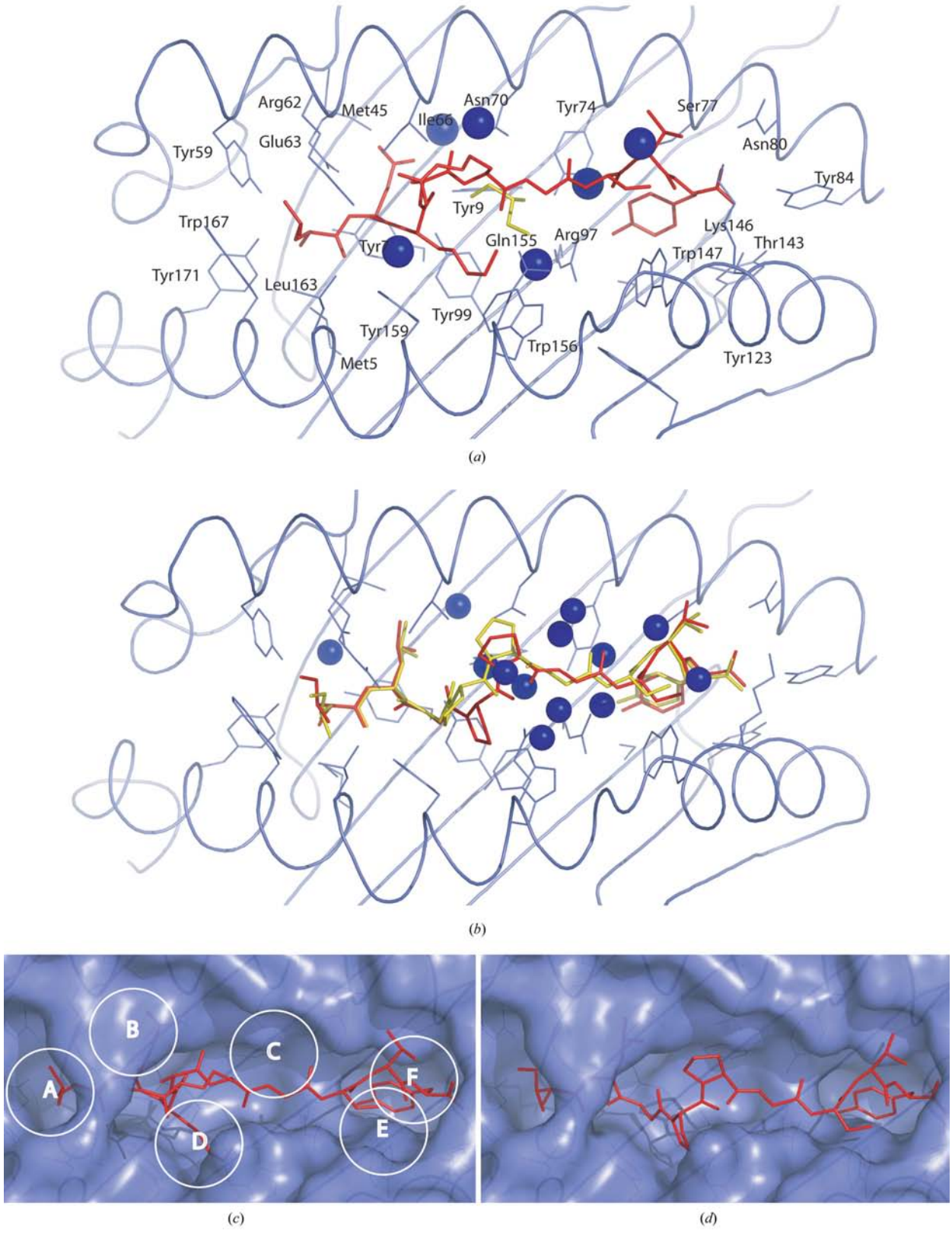

Figure 2
The LEKARGSTY (*a*, *c*) and ILGPPGSVY (*b*, *d*) peptides located in the binding groove of HLA-B*1501. (*a*, *b*) A carbon-α trace of the HLA-B*1501 α_1/α_2-domain and water molecules (spheres) are shown in blue. Selected MHC-I residues important for peptide binding are represented by thin sticks. The LEKARGSTY peptide is shown in red. The glycerol molecule in the LEKARGSTY structure is shown in yellow stick representation and is located below the peptide. The A- and B-conformations of the ILGPPGSVY peptide are shown in red and yellow, respectively. (*c*, *d*) The peptides are shown in a surface representation of the HLA-B*1501 binding groove. Peptide binding pockets are indicated by circles in (*c*).

peptide) were pooled and concentrated on a 10 kDa spin filter to 2.1 mg ml^{-1} (48 μ*M*) (LEKARGSTY) and 3.8 mg ml^{-1} (87 μ*M*) (ILGPPGSVY).

2.5. Crystallization and data collection

Crystals of the two HLA-B*1501 complexes were grown using the hanging-drop technique. Buffers from both Crystal Screen 1 and 2 (Hampton Research) were used, where 0.5 ml was applied to the reservoir and subsequently 1 μl of buffer was mixed with 1 μl of protein solution. Initially, the experiments were set up at 293 K. Since no crystals appeared after 2 months, the plates were then incubated at 277 K. LEKARGSTY crystals appeared in a droplet containing 200 m*M* magnesium acetate tetrahydrate, 100 m*M* sodium cacodylate (pH 6.5) and 20%(*w*/*v*) PEG-8000 from Crystal Screen 1. ILGPPGSVY crystallized under the conditions 200 m*M* ammonium acetate, 0.1 *M* tri-sodium citrate dihydrate (pH 5.6) and 30%(*w*/*v*) PEG-4000. LEKARGSTY data were collected at the I911-5 beamline at MAX-lab, Lund, Sweden and ILGPPGSVY data were collected at the BW7B EMBL/DESY beamline in Hamburg, Germany. Both complexes crystallize in space group $P2_12_12_1$ with one complex per asymmetric unit, see Table 1. Intensities were integrated with *MOSFLM* (Powell, 1999) and scaled with *SCALA* (Evans, 2006).

2.6. Structure determination and refinement

The LEKARGSTY complex structure was solved by molecular replacement with *MolRep* (Vagin & Teplyakov, 2000) using HLA-B*5301 (PDB code 1a1m) as the initial model. An initial model consisting of the HLA-B*1501 heavy chain and β_2m was automatically built with *ARP/wARP* (Cohen *et al.*, 2004) and residue side chains were substituted using *guiSIDE* (Cohen *et al.*, 2004). Multiple rounds of manual inspection and rebuilding in the program *O* (Jones *et al.*, 1991) were performed followed by restrained refinements in *REFMAC*5 (Murshudov *et al.*, 1997). This included the manual building of the LEKARGSTY peptide. The final structure contains the HLA-B*1501 residues 1–274, the β_2m residues 1–99, LEKARGSTY peptide, one PEG-8000 fragment, one urea, two glycerol and 225 water molecules ('a', 'b' or 'p' in front of a residue meaning the MHC-I α-chain, the β_2m chain or the bound peptide, respectively).

Since the ILGPPGSVY complex crystallized with the same unit cell and space group as the LEKARGSTY complex, the structure was solved by difference Fourier methods and rigid-body refinement. The final model was obtained through multiple rounds of manual inspection in the program *O* followed by restrained refinements in *REFMAC*5. The pPro4-pPro5 residues of the ILGPPGSVY peptide were built in two different conformations (Fig. 1). Firstly, the two ILG and GSVY peptide segments were built into a difference electron-density map with subsequent refinement in *REFMAC*5. Secondly, two separate conformations of the pPro4-pPro5 segment were built separately by multiple rounds of manual rebuilding followed by restrained refinements in *REFMAC*5. The final structure consists of the HLA-B*1501 residues 1–274, the β_2m residues 1–99, the ILGPPGSVY peptide, two sulfate ions, one urea, one glycerol and 595 water molecules. Additional refinement statistics are given in Table 1. Both structures have been deposited at the RCSB Protein Data Bank with PDB accession codes 1xr8 and 1xr9. All figures were prepared with *PyMOL* (DeLano, 2006).

2.7. Peptide binding experiments

The binding affinities of the LEKARGSTY and ILGPPGSVY peptides to HLA-B*1501 were measured as previously described (Sylvester-Hvid *et al.*, 2002). Briefly, 2 n*M* denatured HLA-B*1501 heavy chain was *de novo* folded in 20 m*M* Tris–maleate (pH 6.6) in the presence of 100 n*M* β_2m and a series of fivefold dilutions of the peptides starting at 20 μ*M*. The folded MHC-I molecules were captured with the W6/32 mAb, and detected by HRP-conjugated P174 mAb directed against β_2m. TMB was added as a substrate for HRP and after reaction the OD_{450} was measured. Using HLA-A*0201 as an internal assay standard, the OD_{450} values were converted to n*M* concentrations. The affinities were calculated based on the concentrations of peptide offered and resulting complexes formed using one-site hyperbola curve-fitting of the *Prism* (GraphPad) statistical package.

3. Results

The binding affinities of the LEKARGSTY and ILGPPGSVY peptides to HLA-B*1501 were determined to 200 n*M* and 70 n*M*, respectively. Thus, both peptides bind to HLA-B*1501 with an affinity stronger than 500 n*M*, which is currently believed to be the limit for eliciting a CTL response (Sette *et al.*, 1994).

The crystal structures of HLA-B*1501 in complex with the two peptides LEKARGSTY and ILGPPGSVY were determined at 2.3 and 1.8 Å resolution, respectively. The two HLA-B*1501 structures are found to have the expected overall structure as seen in all previous MHC-I structures (Madden, 1995). Indicators of the quality of the structures are given in Table 1. The crystal packings do not directly affect the peptides in the MHC-I binding groove (not shown); hence, the peptide conformations are most probably only because of contact with MHC-I residues, glycerol and water molecules located in the peptide binding groove. The MHC-I binding groove can be divided into different pockets (A to F), in which the peptide residues bind (Matsumura *et al.*, 1992; Saper *et al.*, 1991). The peptide termini in both HLA-B*1501 complexes are tethered to conserved amino-acid residues in the A-, B- and F-pockets, see Fig. 2. MHC-I residues implicated in the binding of the LEKARGSTY and ILGPPGSVY peptides are listed in Tables 2 and 3. Several of the MHC-I residues listed are conserved among the different alleles and adopt similar rotamer conformations. Furthermore, structural alignment did not show any significant rotamer conformation differences of residues located in the peptide binding groove between the

Table 2
LEKARGSTY peptide contacts to HLA-B*1501.

The hydrogen-bond cut-off is 3.6 Å.

LEKARGSTY		Potential hydrogen-bond partner			van der Waals contacts
Residue	Atom	Residue	Atom	Distance (Å)	
pLeu1	N	aTyr7	OH	2.9	aTyr59, aArg62, aGlu63, aLeu163, aTrp167
	N	aTyr171	OH	2.6	
	O	aTyr159	OH	2.6	
pGlu2	N	aGlu63	OE1	3.1	aTyr7, aTyr9, aMet45, aGlu63, aIle66
	O	aArg62	NH2	3.1	
	OE1	aGlu63	OE1	2.7	
	OE1	aGlu63	O	3.6	
	OE2	aTyr9	OH	2.7	
	OE2	aGlu63	OH	2.7	
	OE2	W25	OW	2.6	
pLys3	N	aTyr99	OH	3.2	aGln155, aTrp156, aTyr159
	O	GOL3002	O3	2.9	
	NZ	pArg6	O	2.4	
	NZ	GOL3002	O1	3.5	
	NZ	W95	OW	2.7	
pAla4	N	W85	OW	3.3	pArg5
	O	W79	OW	3.0	
pArg5	O	pLys3	NZ	2.4	
	O	GOL3002	O1	3.0	
pGly6	O	W41	OW	3.5	
pSer7	N	aGlu152	OE2	3.4	
	OG	pThr8	N	2.5	
	OG	pThr8	O	2.8	
	OG	W203	OW	3.1	
pThr8	N	pSer7	OG	2.5	aThr73, aGlu76
	N	pThr8	OG1	2.8	
	O	pSer7	OG	2.8	
	O	pThr8	OG1	3.0	
	O	aLys146	NZ	3.3	
	O	aTrp147	NE1	3.2	
	OG	aLys146	NZ	2.6	
pTyr9	N	aSer77	OG	2.9	aTyr74, aLeu81, aLeu95, aTyr123, aThr143, aTrp147
	O	aAsn80	ND2	2.9	
	OXT	aTyr84	OH	3.2	
	O	aLys146	NZ	2.5	
	OH	aArg97	NH1	3.5	
	OH	aSer116	OG	2.6	

two HLA-B*1501 structures except for aGlu152, which is discussed below.

3.1. The A-pocket

The A-pocket has a mouth opening towards the TCR binding site, where charged and aliphatic residues may protrude into this opening and interact with peripheral parts of the TCR. The bottom of the A-pocket is hydrophobic because of the aMet5 pointing directly toward the peptide N-terminus. However, the B-pocket part proximal to the A-pocket is hydrophilic because of the aTyr159 hydroxyl group pointing toward the carboxy oxygen of the P1 residues. Furthermore, the α_1-helix proximal side of the A-pocket is also hydrophilic because of the hydroxyl groups of aTyr7 and aTyr171 pointing in the direction of the peptide N-terminus. The peptide N-terminal backbone N atoms make canonical hydrogen bonds with the conserved aTyr7 and aTyr171 residues (Tables 2 and 3) as observed in most present MHC-I structures with a bound nonamer peptide (Madden, 1995). Furthermore, aTyr7 and aTyr59 form hydrogen bonds to a deeply buried water molecule (W18 in LEKARGSTY and W7 in ILGPPGSVY, see Fig. 2) conserved in nearly all MHC-I structures (Ogata & Wodak, 2002). The two lateral α-helices encapsulating the peptide binding groove are stabilized by a hydrogen bond between aTyr59 and aTyr171. The upper region of the A-pocket is hydrophobic caused by the lining of aliphatic/aromatic parts of aTyr59, aArg62, aGlu63, aLeu163 and aTrp167 residues, see Fig. 2.

Thus, this pocket may accommodate hydrophobic P1 side chains such as Ala, Leu or Ile. The HLA-B*1501 structures reported here both have hydrophobic residues (pLeu1/pIle1) in the P1 position. On the other hand, larger side chains such as Asp, Glu, Lys or Arg having a distal charge have also been reported (Krüger *et al.*, 2005; Rammensee *et al.*, 1999). In summary, the majority of the A-pocket is hydrophobic caused by the aTyr59, aLeu163 and aTrp167 residues. This explains why HLA-B*1501 prefers hydrophobic residues at P1.

3.2. The B-pocket

P2 and P9 residues are primary anchors in most nonamer peptides, meaning that these particular peptide residues are 'tethered' directly to the HLA alleles (Kubo *et al.*, 1994; Yamada *et al.*, 1999). Peptide P2 side chains bind to MHC-I in the B-pocket, and thus the chemical environment in the B-pocket of MHC-I is a major determinant for the peptide binding specificity. Multiple MHC-I residues are involved in shaping the chemical environment in the B-pocket (Tables 2 and 3). The outer part of this pocket is shaped by aTyr7, aTyr9, aArg62, aGlu63 aIle66 and aTyr99 (Figs. 2 and 3, and Table 4). aTyr7 is located on the first β-strand in the α_1-domain creating a hydrophobic environment at the floor promixal to the mouth of the B-pocket. aMet45 and aIle66 are located on the helix in the α_1-domain and thus render the upper part of the B-pocket hydrophobic as well. The sides are hydrophilic because of aArg62, aGlu63 and aTyr99. The back of the B-pocket is also hydrophilic caused by the aSer67 hydroxy group.

In both HLA-B*1501 structures, the peptide binding in this pocket is stabilized by a hydrogen bond from the aArg62 NH atoms to the P2 peptide backbone carbonyl O atoms. aArg62 and aIle66 together shield off the P2 residue from recognition

Table 3
ILGPPGSVY peptide contacts to HLA-B*1501.

The hydrogen-bond cut-off is 3.6 Å.

ILGPPGSVY		Potential hydrogen-bond partner			van der Waals contacts
Residue	Atom	Residue	Atom	Distance (Å)†	
pIle1	N	aTyr7	OH	3.3/2.8	aMet5, aTyr7,
	N	aTyr171	OH	2.8/2.6	aTyr59, aArg62,
	O	aTyr159	OH	2.7/2.5	aGlu63, aTrp167
pLeu2	N	aTyr7	OH	3.5/3.6	aTyr7, aTyr9,
	N	aGlu63	OE2	2.7/2.9	aMet45, aGlu63,
	O	aArg62	NH1	3.4/2.9	aIle66
	O	aArg62	NH2	– /3.3	
pGly3	N	aTyr99	OH	2.7/3.1	pPro4, aTyr99,
	O	W16	OW	3.2/2.8	aTyr159
pPro4	O	W518	OW	3.1/–	pPro4, pPro5,
	O	W558	OW	2.5/3.5	aGln155, aTrp156,
	O	W570	OW	3.0/–	aTyr159
pPro5	O	aGln155	NE2	2.7/3.6	pPro4, aIle66,
	O	W143	OW	2.7/2.6	aThr69
pGly6	N	W112	OW	3.3/3.1	
	O	W194	OW	–/3.6	
	O	W541	OW	3.0/2.7	
pSer7	N	aGlu152‡	OE1	3.5/3.4	aTrp147, aGlu152‡
	N	aGlu152‡	OE2	2.6/2.6	
	O	W51	OW	2.9/2.7	
	O	W194	OW	3.1/2.6	
	OG	pVal8	O	2.8/2.8	
	OG	aTrp147	NE1	3.6/–	
	OG	W200	OW	2.7/2.7	
pVal8	N	W94	OW	2.9/2.9	aGlu76, aSer77
	O	pSer7	OG	2.8/2.8	
	O	aTrp147	NE1	3.1/2.9	
pTyr9	N	aSer77	OG	2.9/3.0	aTyr74, aSer77,
	O	aAsn80	ND2	2.8/3.2	aLeu81, aTyr123,
	O	aLys146	NZ	2.9/2.8	aThr143, aTrp147
	OXT	aTyr84	OH	2.5/2.8	
	OXT	aThr143	OG1	2.8/2.6	
	OH	aArg97	NH1	3.3/3.2	
	OH	aSer116	OG	2.4/2.8	

† Distance to the A/B-conformation of the ILGPPGSVY. ‡ The B-conformation of the given residue.

by the TCR as shown in Figs. 2(*c*) and 3. Similar to other MHC-I structures (Ogata & Wodak, 2002) a partially conserved water molecule (W25 in Fig. 2*a*) is bound deeply in the B-pocket by aTyr9, aSer67 and aAsn70. In the LEKARGSTY complex, the pGlu2 γ-carboxylate makes a potential fourth hydrogen bond to the W25 water molecule. This additional hydrogen bond is not present in the ILGPPGSVY complex owing to the hydrophobic nature of pLeu2.

In summary, the B-pocket is relatively large because of the small aSer67 residue located at the bottom. Most of the pocket interior is hydrophobic which is consistent with P2 anchor residue preference for Gln and Leu as described previously (Falk *et al.*, 1995; Barber *et al.*, 1996; Prilliman *et al.*, 1997). The specificity of the B-pocket is thus most importantly determined by the aMet45, aGlu63, aIle66 and aSer67 residues creating a hydrophobic environment.

3.3. The C- and D-pockets

The C- and D-pockets are the most solvent-exposed pockets in the HLA-B*1501 and are located in the center of the peptide binding groove. The two pockets are primarily constituted by

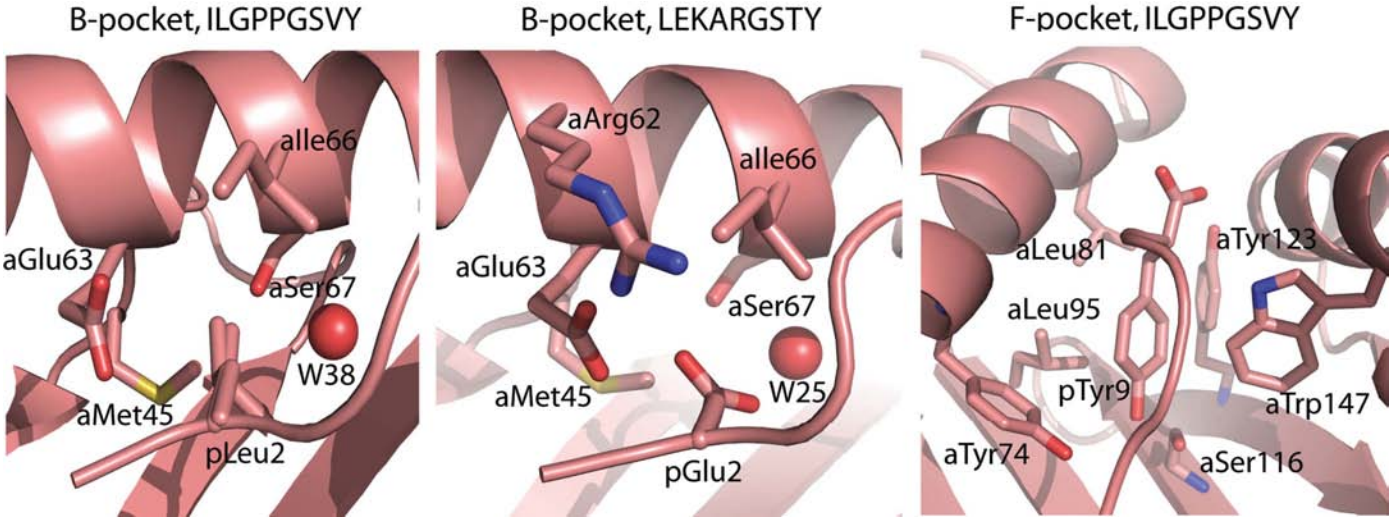

Figure 3
Detailed view of the B- and F-pockets. HLA-B*1501 believed to be important in shaping the peptide binding specificity of peptide positions 2 and 9 are shown. A view of the ILGPPGSVY F-pocket structure is omitted since the peptides in both structures have a tyrosine in position 9.

Table 4
HLA supertype-associated amino-acid motifs.

Allele†	Supertype‡	P2§	P9§
A*01¶	A1	T, S	Y
A*0201	A2	L, M	V, L
A*1101	A3	Y, T	K
B*3501	B7	P, V	L, Y
B*0801††	B8	N.d.‡‡	L
B*2705	B27	R	L, F
B*4402	B44	E	F, L
B*1501	B62	Q, L	Y, V

† Allele chosen based on present structures. ‡ Allele belongs to supertype [according to Lund *et al.* (2004)]. § Amino-acid motif [according to Lund *et al.* (2004)]. ¶ No explicit HLA-A*0101 allele was found, and data for HLA-A*01 was used instead. †† No consensus at P9, but at P4 instead. ‡‡ Not determined.

aIle66, aTyr99, aGln155, aTrp156 and aTyr159 resulting in a hydrophobic environment. The flat and open form allows the accommodation of larger peptide residues such as the pLys3 seen in the LEKARGSTY complex. pLys3 makes hydrophobic contacts to aGln155, aTrp156 and aTyr159 situated on the surrounding α_2-helix. In the LEKARGSTY complex, the pAla4 and pArg5 point away from the floor in the peptide binding groove and towards the location of the antigen recognizing CDR3-loops in a potential T cell receptor. In contrast to this, two consecutive proline residues, pPro4 and pPro5, in the ILGPPGSVY complex point in a horizontal and upward direction, respectively (Fig. 2). The pPro4 residue adopts two different conformations in the peptide binding groove, and primarily makes hydrophobic contacts to aGlu155, aTrp156 and aTyr159. The pPro4 residue in the A-conformation of the ILGPPGSVY peptide seems to be closer to aTrp156, whereas pPro4 in the B-conformation is closer to aTyr159. aIle66, which plays a major role in the B-pocket specificity, is also implicated in hydrophobic interactions with pPro5 in both ILGPPGSVY peptide conformations. pPro5 is 1 Å closer to aIle66 in its B-conformation. pPro5 also makes weak hydrophobic interactions with aThr69 in the α_1-helix.

In summary, the C- and D-pockets are very flat and solvent exposed. Because of this, medium or large hydrophobic peptide residues fit best into these pockets as previously observed (Rammensee *et al.*, 1999). The hydrophobic environment is made from the aIle66, aThr69, aGln155, aTrp156 and aTyr159 residues.

3.4. The E-pocket

Peptide P6 residues bind to residues in the proximity of the E-pocket. In both the LEKARGSTY and ILGPPGSVY complexes, the P6 residue is a glycine. Since pGly6 lacks a side chain, this enables a region of the peptide around this residue to be close to the α_2-helix. The peptide main chain is elevated above the floor of the binding groove, allowing the presence of several water molecules in this region. These water molecules are acting as bridging molecules between the peptide backbone and HLA-B*1501 residues. In the LEKARGSTY

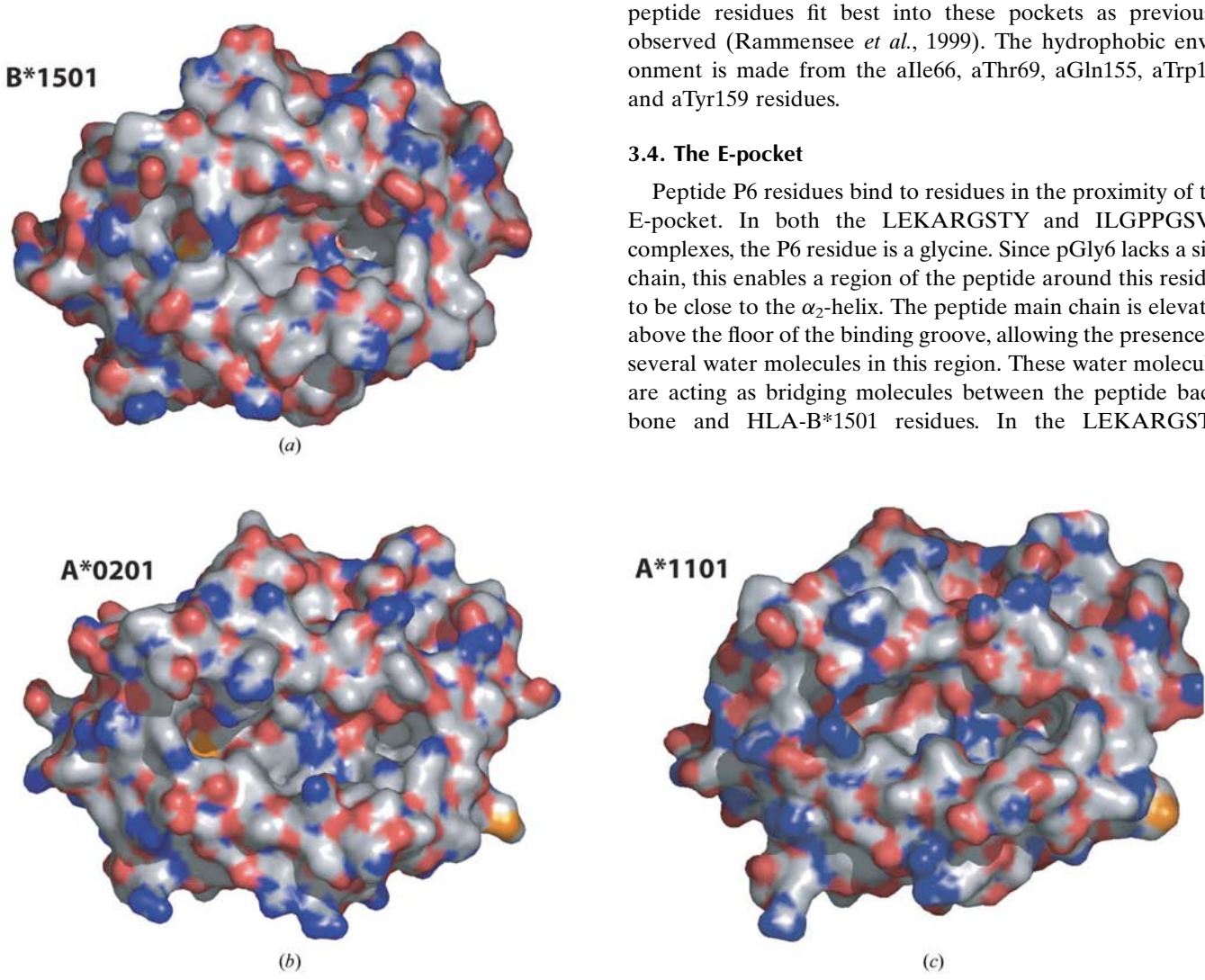

Figure 4
Surface representations of (*a*) HLA-B*1501 (this work), (*b*) HLA-A*0201 (Khan *et al.*, 2000) and (*c*) HLA-A*1101 (Blicher *et al.*, 2005). The surfaces are colored by the standard convention for atoms.

complex, a glycerol molecule (GOL3002) is replacing the role of some water molecules. No direct interactions of the pGly6 with the HLA-B*1501 side chains are present. aGly152 is found in two conformations leaving little space to a potential peptide P6 side chain.

The residues lining the E-pocket are aLys146, aTrp147 and aGlu152, and are all located on the α_2-helix. The aromatic/aliphatic part of these residues renders the E-pocket very hydrophobic and its location is elevated compared with the other five pockets. The elevation is caused by the big aTrp147 residue located beneath the side chain of P7 residues. In both structures presented here, the side chain of aTrp147 is perpendicular to the bottom of the E-pocket, which makes it unable to engage in aromatic stacking with a potential aromatic peptide P7 residue. The LEKARGSTY pSer7 is not involved in hydrogen bonding, whereas the ILGPPGSVY pSer7 is slightly closer to the α_2-helix and forms a hydrogen bond to aTrp147. The LEKARGSTY pThr8 makes a hydrogen bond to the aforementioned aLys146.

In summary, the E-pocket is very flat and hydrophobic, which enables it to be a place holder for aliphatic amino acids, such as Val, Leu, Ile and Met (Rammensee *et al.*, 1999). The HLA-B*1501 residues conferring this specificity are aLys146, aTrp147 and aGlu152.

3.5. The F-pocket

The F-pocket binds the C-terminal residue side chain of the peptide, which is the primary anchor residue for peptide binding to HLAs belonging to the B62 supertype among others (Prilliman, Jackson *et al.*, 1999). This pocket extends deeply towards the floor of the peptide binding groove of HLA-B*1501 as shown in Figs. 2 and 3. The peptide C-terminal carboxy group is located just above the entrance to the F-pocket. Here, it is involved in a network of conserved hydrogen bonds to aAsn80, aTyr84, aThr143 and aLys146. These residues are distributed on both α-helices and the aTyr84 seals off this end of the peptide binding groove between these α-helices. The aAsn80 and aLys146 reach from each of their respective helices towards each other above the C-terminal end of the peptide. In this way, they shield off the C-terminus part of the peptide from the solvent and a potential T-cell receptor.

The entrance of the F-pocket (the region that is actually beneath the P8 residue) is hydrophilic towards the α_1-helix because of aArg97 located at the floor of the peptide binding groove and this residue points up towards the peptide main chain. The α_2-helix proximal part of the F-pocket entrance is partly hydrophilic because of the N atom in aTrp147. The F-pocket itself is quite large and capable of containing the aromatic residues Tyr, Phe and in some cases Trp. The majority of the internal surface of the F-pocket is hydrophobic because of the surrounding aliphatic and aromatic HLA-B*1501 residues. The bottom of the pocket is slightly hydrophilic due to aSer116, which forms a hydrogen bond with the hydroxy group of pTyr9. The aforementioned aArg97 also creates a hydrophilic region and may be engaged in hydrogen bonding to the pTyr9 hydroxy group. The rest of the F-pocket is hydrophobic and is lined by the aTyr74, aLeu81, aLeu95, aTyr123, aThr143 and aTrp147 HLA-B*1501 residues. The aTrp147 that is also involved in shaping the specificity of the E-pocket and partially also the aThr143 make up the α_2-helix proximal hydrophic interior of the F-pocket. The aromatic plane of the aTrp147 is perpendicular to that of pTyr9. This is also true for the aTyr123 aromatic plane. Hence, the binding of pTyr9 in the E-pocket does not get a contribution from aromatic stacking of peptide and HLA-B*1501 residues.

The residues most important for the specificity of the HLA-B*1501 F-pocket are aTyr74, aLeu81, aLeu95, aSer116, aTyr123 and aTrp147. These residues are responsible for the hydrophic interior of the F-pocket and their spatial arrangement makes the pocket capable of containing large, bulky peptide side chains. At the bottom of the F-pocket is located the small aSer116, which may act as a hydrogen-bond partner. In other alleles Tyr is found at this position. This is an important difference as it allows HLA-B*1501 to contain large, bulky peptide side chains such as the highly favored Tyr residue.

4. Discussion

Here, we present the first two structures of any current member of the B62 supertype. The structures have been determined of HLA-B*1501 in complex with an antigenic peptide from the Epstein–Barr virus EBNA-3A protein (LEKARGSTY) (Rickinson & Moss, 1997) and an autologous peptide (ILGPPGSVY) (Barber *et al.*, 1997; Prilliman, Jackson *et al.*, 1999), respectively. The peptides in both complexes adopt a canonical backbone conformation seen in most MHC-I structures with a bound nonamer peptide (Madden, 1995). The peptide N-terminus is tightly bound in the HLA-B*1501 A- and B-pockets, whereas the peptide C-terminal pTyr9 residue is deeply anchored in the F-pocket. The overall structures of the peptide backbones are similar to those of previously observed nonamer peptides in complex with HLA-A*0201 and others (Madden, 1995). The central part of the peptides is elevated from the peptide binding groove towards the CDR3 loop of a potential T cell receptor. The pArg5 side chain in the LEKARGSTY peptide actually points directly away from the HLA-B*1501 peptide groove floor and is fully solvent exposed. Large residues at this position in the peptide are believed to be important for the cytotoxic T-cell reponse toward an antigenic peptide (Barber *et al.*, 1997). The large side chain of pArg5 in the LEKARGSTY complex might increase the interaction with the CDR3 region of the T-cell receptor in the same way as seen with the MW-peg in the MHC/TCR structure (Chen *et al.*, 2005).

Some peptide residues are bound more tightly to HLA-B*1501 than others. The most important anchor residues of peptides binding to this HLA allele are P9 which binds to the HLA-B*1501 F-pocket as well as P2 which binds to the B-pocket (see Table 4). P9 peptide residues such as Phe, Trp and Tyr have previously been determined to be important anchor

residues in peptides binding to HLA-B*1501 and other members of the B62 supertype (Falk *et al.*, 1995; Barber *et al.*, 1996; Prilliman *et al.*, 1997). This is only possible because of the spatial arrangement of the surrounding residues and the hydrophobic interior of the HLA-B*1501 F-pocket.

The residues responsible for the specificity of the F-pocket in HLA-B*1501 are aTyr74, aLeu81, aLeu95, aTyr123 and aTrp147. They create a hydrophobic pocket with a hydrophilic bottom because of the aSer116. This is the ideal environment for a Tyr at P9. It has previously been shown that mutation of aSer116 to aTyr116 in HLA-B*1501 drastically alters the natural bound ligand repertoires (Prilliman, Crawford *et al.*, 1999.). The reason for this may be that aTyr116 sterically hinders binding of large P9 peptide residues.

Major differences in the P9 anchors and F-pocket structures exist between the various HLA supertypes as revealed by a comparison of the A2, A3 and B62 HLA supertypes represented by HLA-A*0201 (Khan *et al.*, 2000), HLA-A*1101 (Blicher *et al.*, 2005) and HLA-B*1501 (this work), respectively. The F-pocket is mostly hydrophobic in all three cases, but the F-pocket of HLA-A*0201 is quite narrow and not so deep compared to those of HLA-A*1101 and HLA-B*1501 (Fig. 4). This is consistent with the observation, that HLA-A*0201 has a peptide P9 anchor preference for smaller, aliphatic amino acids such as Val and Leu, while HLA-A*1101 prefers Lys and HLA-B*1501 prefers Tyr and Val (Rammensee *et al.*, 1999; Lund *et al.*, 2004), see Table 4. The F-pocket dimensions of HLA-B*0801, belonging to the B8 supertype (Lund *et al.*, 2004), are similar to that of HLA-A*0201. HLA-B*0801 especially prefers Leu at P9 (Malcherek *et al.*, 1993; Dibrino *et al.*, 1994). HLA alleles belonging to the A1, B7, B27 and B44 supertypes have preferences for both small P9 residues such as Leu and/or bulky Phe and Tyr residues (DiBrino *et al.*, 1993; Malcherek *et al.*, 1993; Kubo *et al.*, 1994) and are in this context more similar to the B62 supertype than A2 and B8. To emphasize, HLA-B*1501 has a strong preference for Tyr at P9. This is because of the hydrophobic and widely open F-pocket in this allele.

The B-pocket in the peptide binding groove of HLA molecules accommodates the P2 peptide anchor. Most HLA supertypes prefer aliphatic or aromatic peptide residues in the B-pocket (Table 4). However, there are subtle differences; HLA-A*1101 prefers aromatic residues such as Tyr and Phe, whereas HLA-A*0201 and HLA-B*1501 prefer aliphatic residues such as Leu (Rammensee *et al.*, 1999; Lund *et al.*, 2004), see Table 4. In the case of HLA-B*1501 the specificity of the B-pocket is primarily determined by the aMet45, aIle66 and aSer67 residues, which are located on the α_1-helix. Previous studies have shown that the specificity of the B-pocket in HLA-B*1501 is solely determined by an α_1-helical segment (Barber *et al.*, 1997). In contrast, HLA-B*0801 has not been assigned any preferred anchor residues at P2 (Malcherek *et al.*, 1993; Dibrino *et al.*, 1994). The A2, B7 and B62 supertypes prefer small to medium aliphatic P2 residues, whereas the B27 prefers a P2 Arg (Dibrino *et al.*, 1993). A1 and B44 prefer hydrophilic residues such as Thr, Ser and Glu (DiBrino *et al.*, 1993; Kubo *et al.*, 1994).

When sufficient structural information is available for an HLA supertype, this enables us to map common structural and functional features, such as HLA residues playing a major role in peptide specificity. This may be accomplished by structural alignment of a group of HLA structures. The peptide binding groove may then be partitioned according to structural agreement/disagreement (determined by calculated RMSD values) or *B*-factor similarities/discrepancies. A more detailed understanding of the structural aspects of HLA side chains would also support the development of prediction tools that may enable us to predict whether a peptide binds to an HLA molecule or not (Bordner & Abagyan, 2006; Bui *et al.*, 2006). In best cases, quantitative data can be derived and eventually correlated with biochemically measured dissociation constants for a given peptide–HLA complex. However, a major challenge is to obtain structural information on all the other HLA supertypes. In addition, multiple structures within each HLA supertype are necessary for accurate structural prediction of the peptide docking in the HLA peptide binding groove. Finally, the complex network of water molecules, directly or indirectly involved in the peptide binding, should be understood in detail (Fagerberg *et al.*, 2006). This, in turn, requires high-resolution structures of different peptide–HLA complexes as well as molecular dynamics simulations to model the locations and trajectories of moving water molecules.

Anja Gjol and Stine Johansen are thanked for performing the peptide binding experiments. This work was funded by the Danish Centre for Synchrotron Radiation (DANSYNC), EU 6FP 503231 and NIH HHSN266200400025C.

References

Barber, L. D., Percival, L., Arnett, K. L., Gumperz, J. E., Chen, L. & Parham, P. (1997). *J. Immunol.* **158**, 1660–1669.
Barber, L. D., Percival, L., Valiante, N. M., Chen, L., Lee, C., Gumperz, J. E., Phillips, J. H., Lanier, L. L., Bigge, J. C., Parekh, R. B. & Parham, P. (1996). *J. Exp. Med.* **184**, 735–740.
Blicher, T., Kastrup, J. S., Buus, S. & Gajhede, M. (2005). *Acta Cryst.* D**61**, 1031–1040.
Bordner, A. J. & Abagyan, R. (2006). *Proteins*, **63**, 512–526.
Bui, H.-H., Schiewe, A. J., von Grafenstein, H. & Haworth, I. S. (2006). *Proteins*, **63**, 43–52.
Chen, J.-L., Stewart-Jones, G., Bossi, G., Lissin, N. M., Wooldridge, L., Choi, E. M. L., Held, G., Dunbar, P. R., Esnouf, R. M., Sami, M., Boulter, J. M., Rizkallah, P., Renner, C., Sewell, A., van der Merwe, P. A., Jakobsen, B. K., Griffiths, G., Jones, E. Y. & Cerundolo, V. (2005). *J. Exp. Med.* **201**, 1243–1255.
Christensen, J. K., Lamberth, K., Nielsen, M., Lundegaard, C., Worning, P., Lauemller, S. L., Buus, S., Brunak, S. & Lund, O. (2003). *Neural Comput.* **15**, 2931–2942.
Cohen, S. X., Morris, R. J., Fernandez, F. J., Jelloul, M. B., Kakaris, M., Parthasarathy, V., Lamzin, V. S., Kleywegt, G. J. & Perrakis, A. (2004). *Acta Cryst.* D**60**, 2222–2229.
DiBrino, M., Parker, K. C., Shiloach, J., Turner, R. V., Tsuchida, T., Garfield, M., Biddison, W. E. & Coligan, J. E. (1994). *J. Immunol.*, **152**(2), 620–631.
DiBrino, M., Tsuchida, T., Turner, R. V., Parker, K. C., Coligan, J. E. & Biddison, W. E. (1993). *J. Immunol.*, **151**(11), 5930–5935.
DeLano, W. (2006). *PyMOL Home Page*, http://www.pymol.org.
Evans, P. (2006). *Acta Cryst.* D**62**, 72–82.

Fagerberg, T., Cerottini, J.-C. & Michielin, O. (2006). *J. Mol. Biol.* **356**, 521–546.
Falk, K., Rotzschke, O., Takiguchi, M., Gnau, V., Stevanovi, S., Jung, G. & Rammensee, H. G. (1995). *Immunogenetics*, **41**, 165–168.
Ferré, H., Ruffet, E., Blicher, T., Sylvester-Hvid, C., Nielsen, L. L. B., Hobley, T. J., Thomas, O. R. T. & Buus, S. (2003). *Protein Sci.* **12**, 551–559.
Guermonprez, P., Valladeau, J., Zitvogel, L., Thry, C. & Amigorena, S. (2002). *Ann. Rev. Immunol.* **20**, 621–667.
Heemels, M. T. & Ploegh, H. (1995). *Ann. Rev. Biochem.* **64**, 463–491.
Jones, T. A., Zou, J. Y., Cowan, S. W. & Kjeldgaard, M. (1991). *Acta Cryst.* A**47**, 110–119.
Khan, A. R., Baker, B. M., Ghosh, P., Biddison, W. E. & Wiley, D. C. (2000). *J. Immunol*. **164**, 6398–6405.
Krüger, T., Schoor, O., Lemmel, C., Kraemer, B., Reichle, C., Dengjel, J., Weinschenk, T., Mller, M., Hennenlotter, J., Stenzl, A., Rammensee, H.-G. & Stevanovi, S. (2005). *Cancer Immunol. Immunother.* **54**, 826–836.
Kubo, R. T., Sette, A., Grey, H. M., Appella, E., Sakaguchi, K., Zhu, N. Z., Arnott, D., Sherman, N., Shabanowitz, J. & Michel, H. (1994). *J. Immunol.* **152**, 3913–3924.
Lauemøller, S. L., Kesmir, C., Corbet, S. L., Fomsgaard, A., Holm, A., Claesson, M. H., Brunak, S. & Buus, S. (2000). *Rev. Immunogenet.* **2**, 477–491.
Lund, O., Nielsen, M., Kesmir, C., Petersen, A. G., Lundegaard, C., Worning, P., Sylvester-Hvid, C., Lamberth, K., Røder, G., Justesen, S., Buus, S. & Brunak, S. (2004). *Immunogenetics*, **55**, 797–810.
Madden, D. R. (1995). *Annu. Rev. Immunol.* **13**, 587–622.
Malcherek, G., Falk, K., Rötzschke, O., Rammensee, H. G., Stevanovic, S., Gnau, V., Jung, G. & Melms, A. (1993). *Int Immunol.* **5**(10), 1229–1237.
Matsumura, M., Fremont, D. H., Peterson, P. A. & Wilson, I. A. (1992). *Science*, **257**, 927–934.
Murshudov, G. N., Vagin, A. A. & Dodson, E. J. (1997). *Acta Cryst.* D**53**, 240–255.
Ogata, K. & Wodak, S. J. (2002). *Protein Eng.* **15**(8), 697–705.
Powell, H. R. (1999). *Acta Cryst.* D**55**, 1690–1695.
Prilliman, K., Lindsey, M., Zuo, Y., Jackson, K. W., Zhang, Y. & Hildebrand, W. (1997). *Immunogenetics*, **45**, 379–385.
Prilliman, K. R., Crawford, D., Hickman, H. D., Jackson, K. W., Wang, J. & Hildebrand, W. H. (1999). *Tiss. Antigens*, **54**, 450–460.
Prilliman, K. R., Jackson, K. W., Lindsey, M., Wang, J., Crawford, D. & Hildebrand, W. H. (1999). *J. Immunol.* **162**(12), 7277–7284.
Rammensee, H., Bachmann, J., Emmerich, N. P., Bachor, O. A. & Stevanovi, S. (1999). *Immunogenetics*, **50**, 213–219.
Rickinson, A. B. & Moss, D. J. (1997). *Annu. Rev. Immunol.* **15**, 405–431.
Rognan, D., Lauemøller, S. L., Holm, A., Buus, S. & Tschinke, V. (1999). *J. Med. Chem.* **42**(22), 4650–4658.
Saper, M. A., Bjorkman, P. J. & Wiley, D. C. (1991). *J. Mol. Biol.* **219**, 277–319.
Sette, A., Fleri, W., Peters, B., Sathiamurthy, M., Bui, H.-H. & Wilson, S. (2005). *Immunity*, **22**, 155–161.
Sette, A. & Sidney, J. (1999). *Immunogenetics*, **50**, 201–212.
Sette, A., Vitiello, A., Reherman, B., Fowler, P., Nayersina, R., Kast, W. M., Melief, C. J., Oseroff, C., Yuan, L. & Ruppert, J. (1994). *J. Immunol.* **153**, 5586–5592.
Sylvester-Hvid, C., Kristensen, N., Blicher, T., Ferré, H., Lauemøller, S. L., Wolf, X. A., Lamberth, K., Nissen, M. H., Pedersen, L. Ø. & Buus, S. (2002). *Tiss. Antigens*, **59**, 251–258.
Sylvester-Hvid, C., Nielsen, M., Lamberth, K., Røder, G., Justesen, S., Lundegaard, C., Worning, P., Thomadsen, H., Lund, O., Brunak, S. & Buus, S. (2004). *Tiss. Antigens*, **63**, 395–400.
Tscharke, D. C., Karupiah, G., Zhou, J., Palmore, T., Irvine, K. R., Haeryfar, S. M. M., Williams, S., Sidney, J., Sette, A., Bennink, J. R. & Yewdell, J. W. (2005). *J. Exp. Med.* **201**, 95–104.
Vagin, A. & Teplyakov, A. (2000). *Acta Cryst.* D**56**, 1622–1624.
Yamada, N., Ishikawa, Y., Dumrese, T., Tokunaga, K., Juji, T., Nagatani, T., Miwa, K., Rammensee, H. G. & Takiguchi, M. (1999). *Tiss. Antigens*, **54**, 325–332.
Yewdell, J. W., Norbury, C. C. & Bennink, J. R. (1999). *Adv. Immunol.* **73**, 1–77.